Rotational rainbows in the inelastic scattering of N_2 from Au(111)

Keith R Lykke† and Bruce D Kay

Sandia National Laboratories, Albuquerque, NM 87185, USA

Abstract. Resonantly enhanced multi-photon ionization (REMPI) laser spectro-scopic and molecular beam–surface scattering techniques are coupled to study the rotationally inelastic scattering of N_2 from Au(111). The scattered N_2 rotational distributions are markedly non-Boltzmann and exhibit pronounced maxima at large angular momentum transfers ($\Delta J = 20$ to 30). These maxima are indicative of direct rotational rainbow scattering and strongly depend upon the translational energy of the incident N_2 molecular beam. The translational energy dependence of the rainbow rotational energy yields a value of 4.1 kcal mol^{-1} for the depth of the laterally averaged N_2–Au(111) physisorption potential.

1. Introduction

There has been considerable experimental and theoretical interest in gas–surface scattering in recent years and a few reviews [1–3] outline some of the intense activity in the field. Quantum-resolved measurements of the nascent rotational and vibrational distributions of scattered molecules are a sensitive probe of the anisotropies in the gas–surface interaction potential responsible for rotational [4, 5] and vibrational [6] energy transfer. The vast majority of experimental work in this field has involved the scattering of NO from metal, semiconductor and ionic crystal surfaces. In addition to NO, a few other molecular species (HF, CO, I_2, N_2, H_2, HCl, CO_2 and NH_3) have been scattered from single crystal surfaces and detected with quantum-state specificity. In this paper we report the results of a recent experimental study of rotationally inelastic N_2 scattering from Au(111).

2. Experimental details

The experimental apparatus has been described in detail previously [7, 8]. Briefly, a pulsed molecular beam of rotationally cold N_2 is scattered from an Au(111) crystal surface in UHV and detected by (2+1) resonantly enhanced multi-photon ionization (REMPI). The cleanliness and order of the Au(111) target are monitored and preserved using standard surface analytical techniques. The translational energy of the incident N_2 molecular beam is varied by seeding the N_2 in mixtures of H_2, He and Ar. The

† Present address: Argonne National Laboratory, Argonne, IL 60439, USA.

scattered N_2 molecules are detected in a direction orthogonal to the incident beam in the principal scattering plane defined by the incident molecular beam and the Au(111) surface normal. In this configuration, a variety of scattering geometries [7, 8] can be studied by rotating the Au(111) crystal with respect to the incident beam.

Quantum-resolved detection of N_2 is accomplished by $(2+1)$ REMPI of N_2 followed by time-of-flight (TOF) mass spectrometric detection of the photogenerated N_2^+. The $(2 + 1)$ REMPI detection scheme for N_2 is discussed in detail elsewhere [9, 10]. The $\lambda \simeq 200$ nm radiation required for the $(2+1)$ REMPI is produced by frequency tripling a pulsed Nd:YAG pumped dye laser in β-BaB_2O_4 and the approximately 1 mJ/pulse gives a detection sensitivity approaching 10^{-10} torr of 300 K N_2.

3. Results and discussion

The $(2+1)$ REMPI of N_2 employed in this study is approximately 100 times more sensitive than the $(2+2)$ REMPI technique utilized by Sitz *et al* in their elegant studies [11–14] of N_2 scattering from Ag(111), but it has the disadvantage that not all rotational levels are fully resolved. In addition to increased sensitivity, another useful advantage of the $(2 + 1)$ REMPI technique [9, 10], is that for the $a'' \, ^1\Sigma_g^+ \leftarrow X \, ^1\Sigma_g^+$ resonant transition, the Q-branch $(\Delta J = 0)$ gives essentially a direct map of the ground electronic state rotational number density irrespective of any angular momentum alignment or orientation in the laboratory frame. Thus, the $(2+1)$ REMPI spectrum of the scattered N_2 molecules is a direct visual representation of the doubly-differential (final angle and quantum-state) rotationally inelastic scattering cross section. This attractive feature of the $(2+1)$ REMPI technique obviates the need for a complicated polarization analysis [11–14] in extracting rotational populations.

Figure 1 displays three representative spectra taken with the $(2 + 1)$ REMPI technique. The upper panel displays the N_2 rotational distribution for a supersonic molecular beam having a translational energy of 8.0 kcal mol^{-1} and a rotational temperature of approximately 3 K. In this beam only the $J = 0$ ($\sim 66\%$) and $J = 1$ ($\sim 33\%$) rotational states of N_2 are significantly populated. The middle panel in figure 1 displays the spectrum for an 1100 K effusive beam of N_2 with the level $J = 20$ indicated. Notice that the overall spectral envelope is characteristic of a rotational Boltzmann distribution, thus demonstrating the direct mapping nature of the $(2+1)$ REMPI spectroscopic technique. The 2:1 alternation of intensities between even and odd rotational lines arises from the Bose–Einstein nuclear spin statistics of $^{14}N_2$. The bottom panel in figure 1 displays the spectrum for a 8.0 kcal mol^{-1} supersonic beam of N_2 scattered from a 300 K Au(111) surface. The incident beam angle is 30° with respect to the Au(111) surface normal and the scattering is detected in the superspecular direction 60° from the surface normal. As is clearly evident from a cursory visual comparison of the incident and scattered spectra the scattering is rotationally inelastic. Additionally, the scattered rotational distribution is markedly non-Boltzmann as evidenced by the pronounced bimodality of the rotational envelope. The local maximum at $J = 22$ is an unambiguous spectral signature of inelastic rotational rainbow scattering [1, 15, 16].

By analogy with elastic rainbow scattering, inelastic rotational rainbows [1, 15, 16] arise when the excitation function, $J_f(\gamma)$, exhibits an extremum with respect to the orientation angle γ. The orientation angle, γ, is defined as the angle between the molecular axis and the surface normal. Classically, an initially non-rotating molecule

incident with $\gamma = 0$ or $\gamma = \pi/2$ will have a final scattered angular momentum $J_f = 0$ by symmetry. For intermediate values of γ the rotational excitation will be non-zero and will be described by some function $J_f(\gamma)$ *which must go through at least one maximum*, as γ is increased from 0 to $\pi/2$. The excitation function for a homonuclear molecule like N_2 will exhibit a single maximum at $\gamma \simeq \pi/4$.

Detection of inelastically scattered N_2 at different final scattering angles results in drastically different rotational energy distributions [17]. Molecules scattered into superspecular final angles (i.e. exiting closer to the surface than specular) show large rotational energy transfer and pronounced rainbow features, while subspecular detection (i.e. closer to the surface normal than specular) results in nearly rotationally elastic scattering. In the parlance of scattering, these measurements reflect differences in the doubly-differential rotationally inelastic scattering cross section. The observed [17] dependence of the scattered rotational distribution upon final scattering angle indicates that the forces that give rise to rotational excitation act predominantly perpendicular to the surface plane. In other words, the linear momentum of the N_2 molecule parallel to the surface plane is nearly conserved during the collision. Thus, those molecules for which a translational-to-rotational (T-R) energy transfer occurs are scattered into larger final angles than those which scatter without a T-R transfer. Additional dynamical information can be obtained by examining the dependence of the rotationally resolved angular distributions upon incident beam translational energy, incident angle and surface temperature. A discussion of these dependences will appear in a future publication [17].

Figure 2 displays $(2 + 1)$ REMPI spectra of N_2 superspecularly scattered from Au(111) at three different incident beam translational energies. These spectra clearly indicate that the angular momentum associated with the rainbow maximum increases with increasing incident translational energy. This observation is in qualitative agreement with classical theories [18-20] of rotational excitation during impulsive molecule-surface scattering. These simple impulsive models predict that the rotational energy associated with the rotational rainbow should scale linearly with the incident normal kinetic energy, E_n. Here E_n is defined as the energy associated with incident linear momentum directed normal to the surface plane, $E_n = E_i \cos^2(\theta_i)$.

Figure 3 displays a plot of the rotational energy of the rainbow, E_r, as a function of E_n of the incident molecular beam. The experimental data are described well by the linear relationship

$$E_r = a(E_n + E_w) \tag{1}$$

with

$$a = 0.288$$
$$E_w = 1.14 \text{ kcal mol}^{-1}.$$

In equation (1) the parameter a is the efficacy for T-R energy transfer for the incident molecular orientation corresponding to the rotational rainbow, and is a measure of the orientational anisotropy of the interaction potential. The parameter E_w is a measure of the laterally averaged attractive potential well depth through which the incident N_2 molecule is accelerated as it approaches the surface. While this is the first quantitative analysis of the dependence of rotational rainbow scattering upon incident translational energy, other studies [8, 21] have found that relationships similar to equation (1)
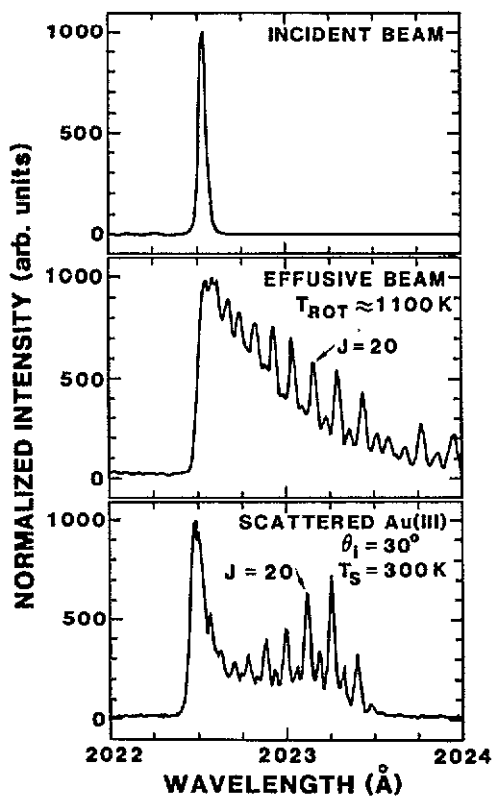
Figure 1. $(2+1)$ REMPI spectra for the incident beam, 1100 K effusive beam, and scattering from a Au(111) surface.
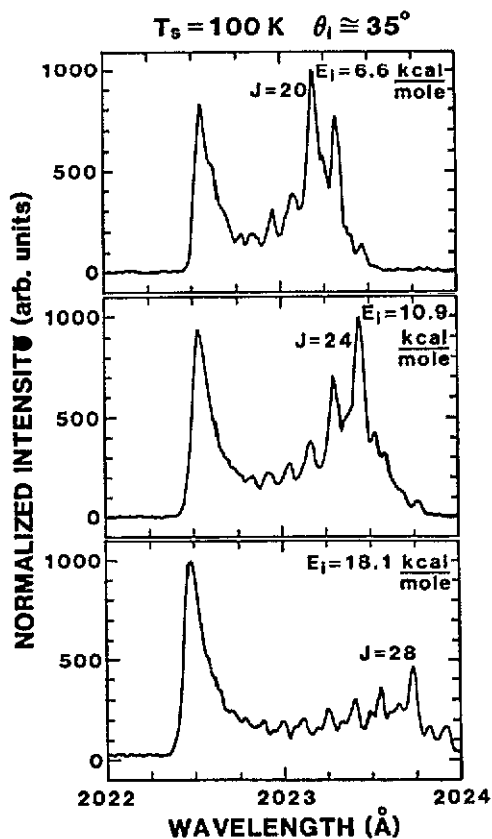
Figure 2. $(2+1)$ REMPI spectra for N_2 scattered from Au(111) at different translational energies.

exist for the average rotational energy transfer observed in rotationally inelastic gas–surface scattering. In those studies, Kubiak *et al* [21], and Lykke and Kay [8] report orientation-averaged well depths of 5.7 and 5.4 kcal mol^{-1} for the NO–Ag(111) and HCl–Au(111) systems, respectively.

The role of the attractive potential in rotational excitation is schematically illustrated in figure 4. As the molecule approaches the surface it is accelerated by the attractive potential until it makes a quasi-impulsive, rotationally inelastic collision with the steep anisotropic repulsive wall of the potential. The rotationally excited molecule is reflected from the surface with a reduced asymptotic translational energy reflecting the T–R energy transfer. For sufficiently large incident translational energies the rotationally inelastic scattering process will only sample continuum levels of the interaction potential. Ignoring dissipative energy transfer to the solid (phonons etc), N_2 molecules having incident normal kinetic energies, $E_n > (a/(1-a))E_w \simeq 1.7$ kcal mol^{-1} will undergo direct inelastic rotational rainbow scattering from Au(111).

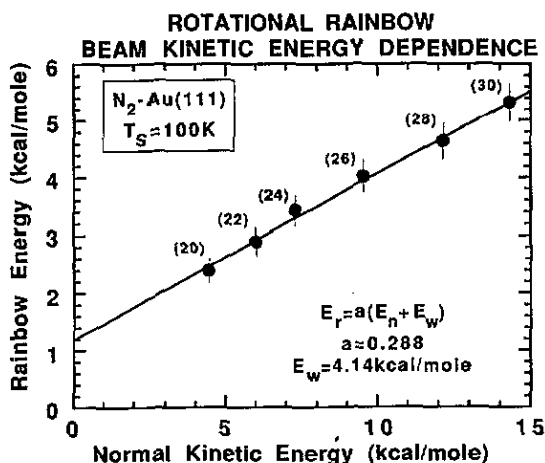**ROTATIONAL RAINBOW**
BEAM KINETIC ENERGY DEPENDENCE

Figure 3. Dependence of rainbow rotational energy upon incident beam normal kinetic energy. Rotational quantum numbers are shown as (J).
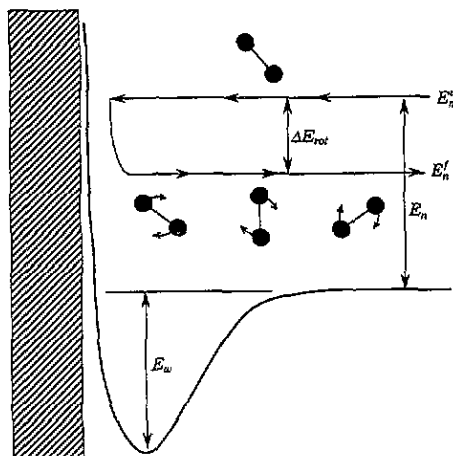

Figure 4. Schematic illustration demonstrating the role of the attractive potential in translational-to-rotational energy transfer.

4. Summary

The following general conclusions can be drawn from this quantum-resolved molecular beam–surface scattering study of rotationally inelastic N_2 scattering from Au(111):

(i) The scattering is strongly dominated by a direct-inelastic mechanism.

(ii) Rotational rainbows are readily observed in the nascent superspecularly scattered rotational state population distribution.

(iii) Translational-to-ratio energy transfer occurs predominantly from forces which act perpendicular to the surface plane.

(iv) The translational energy dependence of the rotational rainbow scattering indicates a value of 4.1 kcal mol^{-1} for the depth of the laterally averaged N_2–Au(111) physisorption potential.

Acknowledgments

References

[1]   Barker J A and Auerbach D J 1984 *Surf. Sci. Rep.* **4** 1
[2]   Lin M C and Ertl G 1986 *Ann. Rev. Phys. Chem.* **37** 587
[3]   King D S and Cavanagh R R 1989 *Adv. Chem. Phys.* **76**
[4]   Kay B D, Raymond T D and Coltrin M E 1987 *Phys. Rev.* B **36** 6695
[5]   Coltrin M E and Kay B D 1988 *J. Chem. Phys.* **89** 551
[6]   Kay B D, Raymond T D and Coltrin M E 1987 *Phys. Rev. Lett.* **59** 2792
[7]   Kay B D and Raymond T D 1986 *J. Chem. Phys.* **85** 4140
[8]   Lykke K R and Kay B D 1990 *J. Chem. Phys.* **92** 2614
[9]   Lykke K R and Kay B D 1989 *J. Chem. Phys.* **90** 7602
[10] Lykke K R and Kay B D 1991 *J. Chem. Phys.* at press
[11] Sitz G O, Kummel A C and Zare R N 1988 *J. Chem. Phys.* **89** 2551В
[12] Sitz G O, Kummel A C, Zare R N and Tully J C 1988 *J. Chem. Phys.* **89** 2572
[13] Kummel A C, Sitz G O, Zare R N and Tully J C 1988 *J. Chem. Phys.* **89** 6947
[14] Kummel A C, Sitz G O, Zare R N and Tully J C 1989 *J. Chem. Phys.* **91** 5793
[15] Barker J A, Kleyn A W and Auerbach D J 1983 *Chem. Phys. Lett.* **97** 9
[16] Kleyn A W 1987 *Commun. At. Mol. Phys.* **19** 133
[17] Lykke K R and Kay B D in preparation
[18] Doll J D 1973 *J. Chem. Phys.* **59** 1038
[19] Nichols W L and Weare J H 1975 *J. Chem. Phys.* **62** 3754
[20] Nichols W L and Weare J H 1977 *J. Chem. Phys.* **66** 1075
[21] Kubiak G D, Hurst J E, Rennagel H G, McClelland G M and Zare R N 1983 *J. Chem. Phys.* **79** 5163